An Efficient Method for Cooperative Multi-Target Localization in Automotive Radar

Xudong Zhang, *Graduate Student Member, IEEE*, Fangzhou Wang, and Hongbin Li, *Fellow, IEEE*

***Abstract*—We consider the problem of locating multiple targets using automotive radar by exploiting a pair of cooperative vehicles, which form a mono- and bi-static sensing system to provide spatial diversity for localization. Each of the two sub-systems can measure the target echoes. The problem is to determine the locations of multiple targets in the surrounding area. A conventional approach is to directly estimate the target locations from the joint distribution of the mono- and bi-static observations, which is computationally prohibitive. In this paper, we propose a efficient two-step method that first uses the delay and angle estimates from each individual system to determine initial target locations, which are subsequently refined via an association and fusion step. Specifically, we use a 2-dimensional (2-D) fast Fourier transform (FFT) based approach to obtain the delay and angle estimates of each target in a sequential manner. The delay/angle estimates obtained by mono-static and bi-static systems lead to two sets of initial target location estimates, which are then sorted and paired via a minimum distance criterion. Finally, the initial location estimates are fused/weighted according to the target strength observed by each system. Simulation results show that our cooperative approach yields significant improved performance over non-cooperative approaches using only the mono-static or bi-static sensing system.**

***Index Terms*—Mono-static sensing, bi-static sensing, multiple targets localization, delay and angle estimation, 2-D FFT.**

I. Introduction

Automotive radar is a rapidly growing civilian radar technology in recent years [1], [2]. Millimeter wave has become the preferred band for short-range vehicle-to-vehicle communication and sensing due to large available bandwidth, which implies high communication throughput and range resolution, as well as the possibility of dense spatial frequency reuse [3]–[5]. While traditional radar aims to detect a relatively small number of objects (e.g., aircrafts), automotive radar operates in complex urban environments and has to simultaneously detect/locate multiple targets in close proximity, which brings some unique signal processing challenges [6]–[10].

Target localization using multiple sensors is a classical problem. A direct method to localize target is the maximum likelihood estimator (MLE) using all sensors' observations [11]. The MLE obtains the target location through a search process over the parameter space and is computationally intensive. Therefore, many prior works pursued an indirect approach by first estimating some location-related parameters, which are then employed to locate the target via a fitting/optimization step. Indirect localization techniques include time-of-arrival (TOA) [12], time-difference-of-arrival (TDOA) [13], direction-of-arrival (DOA) [14] based methods, or combinations of them [15], [16]. Many of these works considered locating a single target in a non-automotive sensing environment.

We consider herein a multi-target localization problem for automotive sensing. An efficient localization method is proposed by using a cooperative mono- and bi-static system comprising a pair of vehicles. In each system, initial target locations are calculated by using the delay and angle estimates obtained by a 2-dimensional (2-D) fast Fourier transform (FFT) approach in a sequential manner. Then, a data association and fusion method is utlized to refine the location estimates via a minimum distance and signal strength based criterion. Simulation results show that the proposed cooperative approach outperforms non-cooperative approaches using only the mono-static or bi-static sensing system.

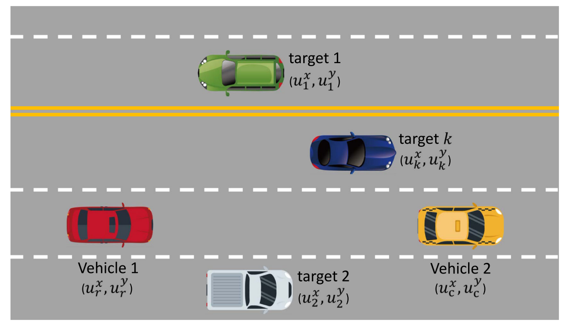

Fig. 1. A cooperative mono-static and bi-static sensing system formed by Vehicles 1 and 2 for multi-target localization.

II. Signal Model

Consider a cooperative automotive sensing scenario depicted in Fig. 1, where Vehicle 1 and Vehicle 2 cooperate in locating multiple targets in the surrounding area. Vehicle 1 acts as a mono-static radar which transmits a probing signal and receives echoes from the environment, while Vehicle 2 acts as bi-static transmitter that sends a probing signal that is known to Vehicle 1 and whose echoes are also received by the latter. In practice, Vehicle 2 could be in communication with Vehicle 1, and the

Manuscript received September 29, 2021; revised October 16, 2021; accepted October 16, 2021. Date of publication October 21, 2021; date of current version January 20, 2022. This work was supported by the National Science Foundation under Grant ECCS-1923739. The associate editor coordinating the review of this manuscript and approving it for publication was Dr. Lu Gan. *(Corresponding author: Hongbin Li.)*

The authors are with the Department of Electrical and Computer Engineering, Stevens Institute of Technology, Hoboken, NJ 07030 USA (e-mail: xzhan24@stevens.edu; fwang11@stevens.edu; hli@stevens.edu).

Digital Object Identifier 10.1109/LSP.2021.3121626

communication signal may serve as the bi-static signal. The purpose is to jointly to exploit the mono- and bi-static probing signals, which offer a geometric diversity in locating the targets.

Suppose Vehicle 1 is located at $\boldsymbol{u}_r = [u_r^x, u_r^y]^T$, while Vehicle 2 is located at $\boldsymbol{u}_c = [u_c^x, u_c^y]^T$. Due to the cooperative relation, we assume $\boldsymbol{u}_r$ and $\boldsymbol{u}_c$ are known, which can be obtained by, e.g., GPS. There are K targets located at $\boldsymbol{u}_k = [u_k^x, u_k^y]^T, k = 1, \ldots, K$, in the surrounding area. For the k-th target, the round-trip propagation delay τ_k^{r} for the mono-static system is

$$\tau_k^r = 2\|\boldsymbol{u}_k - \boldsymbol{u}_r\|/c, \tag{1}$$

and the bi-static propagation delay for the bi-static system is

$$\tau_k^c = (\|\boldsymbol{u}_k - \boldsymbol{u}_r\| + \|\boldsymbol{u}_k - \boldsymbol{u}_c\| - \|\boldsymbol{u}_c - \boldsymbol{u}_r\|)/c, \tag{2}$$

where c is the light of speed. Moreover, the direction of arrival (DOA) angle $\theta_k \in [-\pi/2, \pi/2]$ for the k-th target is the same for the both systems which can be written as

$$\theta_k = \arctan\left(\frac{u_k^y - u_r^y}{u_k^x - u_r^x}\right). \tag{3}$$

We next discuss the signals observed in the two sub-systems.

A. Mono-Static System

Suppose the mono-static sensing system transmits a phased-coded continuous wave (PMCW) $s_r(t)$ within a coherent processing interval [17]

$$s_r(t) = \sum_{l=0}^{L_r-1} \tilde{\boldsymbol{s}}_r[l] g_r(t - lT_{c,r}), \tag{4}$$

where $\{\tilde{\boldsymbol{s}}_r(l)\}_{l=0}^{L_r-1}$ denotes the spreading code with length L_r, $g_r(t)$ the bandlimited chip waveform, and $T_{c,r}$ the chip duration. The receiver receives echoes by using N antennas. The received signal is matched-filtered and sampled at the chirp interval $T_{c,r}$. The received signal at p-th ($p = 1, \ldots, N$) antenna can be written as [18], [19]

$$\tilde{\boldsymbol{y}}_{\mathrm{r},p} = \sum_{k=1}^{K} \alpha_k e^{-j\pi(p-1)\sin\theta_k} \mathbf{F}_r^H \mathbf{W}_r(-\tau_k^r \Delta f_r) \mathbf{F}_r \tilde{\boldsymbol{s}}_r + \tilde{\boldsymbol{n}}_{r,p}, \tag{5}$$

where $\tilde{\boldsymbol{n}}_{r,p}$ is the additive noise vector, α_k the amplitude of the k-th target, and $e^{-j\pi(p-1)\sin\theta_k}$ represents the phase, assuming the antennas form a uniform linear array and the k-th target's DOA is θ_k. In (5), $\mathbf{F}_r$ denotes the L_r-point discrete Fourier transform (DFT) matrix with entries

$$[\mathbf{F}_r]_{l_1,l_2} = e^{-j2\pi(l_1-1)\Delta f_r (l_2-1) T_{c,r}}/\sqrt{L_r}, l_1, l_2 = 1, \ldots, L_r,$$

where $\Delta f_r = 1/(L_r T_{c,r})$ is the sampling spacing in the frequency domain. $\mathbf{W}_r(-\tau_k^r \Delta f_r)$ denotes an $L_r \times L_r$ diagonal matrix with entries

$$[\mathbf{W}_r(a)]_{l,l} = e^{j2\pi(l-1)a}, \quad l = 1, \ldots, L_r. \tag{6}$$

The signal model (5) is flexible and allows non-integer delay τ_k^r with respect to the sampling interval $T_{c,r}$. To see this, note that the waveform $\tilde{\boldsymbol{s}}_r$ is converted to the frequency domain by the DFT matrix $\mathbf{F}_r$, where the continuous delay τ_k^r translates to a phase shift, as imposed by the phase-shifting matrix $\mathbf{W}_r(-\tau_k^r \Delta f_r)$. The phase-shifted waveform is converted back to the time domain via the inverse DFT matrix $\mathbf{F}_r^H$.

For simplicity, let $\boldsymbol{y}_{r,q} = \mathbf{F}_r \tilde{\boldsymbol{y}}_{\mathrm{r},q}$ be the received signal in the frequency domain, and likewise, $\boldsymbol{s}_r = \mathbf{F}_r \tilde{\boldsymbol{s}}_r$ and $\boldsymbol{n}_r = \mathbf{F}_r \tilde{\boldsymbol{n}}_{r,q}$. Then, the received signal in (5) becomes

$$\boldsymbol{y}_{r,p} = \sum_{k=1}^{K} \alpha_k e^{-j\pi(p-1)\sin\theta_k} \mathbf{W}_r(-\tau_k^r \Delta f_r) \boldsymbol{s}_r + \boldsymbol{n}_{r,p}. \tag{7}$$

By stacking the received signals form N antennas as $\boldsymbol{y}_r = [\boldsymbol{y}_{\mathrm{r},1}^T, \ldots, \boldsymbol{y}_{\mathrm{r},N}^T]^T$, the received signal for the automotive radar system can be written as [20]

$$\boldsymbol{y}_r = \mathbf{H}_r \boldsymbol{\alpha} + \boldsymbol{n}_r, \tag{8}$$

where $\boldsymbol{n}_r \in \mathbb{C}^{NL_r \times 1}$ is the complex Gaussian noise vector, $\boldsymbol{\alpha} = [\alpha_1, \ldots, \alpha_K]$, $\mathbf{H}_r = [\boldsymbol{h}_r(\theta_1, \tau_1^r), \ldots, \boldsymbol{h}_r(\theta_K, \tau_K^r)]$ with

$$\boldsymbol{h}_r(\theta_k, \tau_k^r) = (\boldsymbol{a}_{\mathrm{R}}(\theta_k) \otimes \mathbf{W}_r(-\tau_k^r \Delta f_r))\, \boldsymbol{s}_r, \tag{9}$$

and $\boldsymbol{a}_{\mathrm{R}}(\theta_k)$ is the steering vector of the receive phased array for the k-th target

$$\boldsymbol{a}_{\mathrm{R}}(\theta_k) = [1, e^{-j\pi\sin(\theta_k)}, \ldots, e^{-j\pi(N-1)\sin(\theta_k)}]^T. \tag{10}$$

B. Bi-Static System

For the bi-static sensing system, the transmitted PMCW within a symbol period at Vehicle 2 can be written as

$$s_c(t) = \sum_{l=0}^{L_c-1} \tilde{\boldsymbol{s}}_c[l] g_c(t - lT_{c,c}), \tag{11}$$

where $\{\tilde{\boldsymbol{s}}_c\}_{l=0}^{L_c-1}$ denotes the spreading code with length L_c, $g_c(t)$ the bandlimited chip waveform, and $T_{c,c}$ the chip duration employed by Vehicle 2. The transmitted signal $s_c(t)$ is reflected by targets and received by N receive antennas at Vehicle 1. Then the signal is matched-filtered and sampled at the chirp interval $T_{c,c}$. Similar to the mono-static sensing system, the received signal for p-th antenna in the frequency domain can be written as [21]

$$\boldsymbol{y}_{\mathrm{c},p} = \sum_{k=1}^{K} \beta_k e^{-j\pi(p-1)\sin\theta_k} \mathbf{W}_c(-\tau_k^c \Delta f_c) \boldsymbol{s}_c + \boldsymbol{n}_{c,p}, \tag{12}$$

where β_k is the amplitude of the k-th target, $\boldsymbol{n}_c$ the noise, $\boldsymbol{s}_c = \mathbf{F}_c \tilde{\boldsymbol{s}}_c$ the DFT of the spreading code $\tilde{\boldsymbol{s}}_c$ and $\mathbf{F}_c$ the L_c-point DFT matrix. In (12), the $L_c \times L_c$ phase-shifting matrix $\mathbf{W}_c(-\tau_k^c \Delta f_c)$ is diagonal, similarly defined as $\mathbf{W}_r(-\tau_k^r \Delta f_r)$, with Δf_c as the sampling spacing in the frequency domain. Stacking all received signals form N antennas as $\boldsymbol{y}_c = [\boldsymbol{y}_{\mathrm{c},1}^T, \ldots, \boldsymbol{y}_{\mathrm{c},N}^T]^T$, we have [20]

$$\boldsymbol{y}_c = \mathbf{H}_c \boldsymbol{\beta} + \boldsymbol{n}_c, , \tag{13}$$

where $\boldsymbol{n}_c \in \mathbb{C}^{ML_c \times 1}$ is the noise vector, $\boldsymbol{\beta} = [\beta_1, \ldots, \beta_K]$, $\mathbf{H}_c = [\boldsymbol{h}_c(\theta_1, \tau_1^c), \ldots, \boldsymbol{h}_c(\theta_K, \tau_K^c)]$ and

$$\boldsymbol{h}_c(\theta_k, \tau_k^c) = (\boldsymbol{a}_{\mathrm{R}}(\theta_k) \otimes \mathbf{W}_c(-\tau_k^c \Delta f_c))\, \boldsymbol{s}_c. \tag{14}$$

Given observations for both the mono-static sensing system in (8) and bi-static sensing system in (13), the problem of interest is to determine the locations for the K targets.

III. Proposed Two-Step Localization Method

One direct approach to the considered problem is to find the target locations, $\boldsymbol{u}_1, \ldots, \boldsymbol{u}_K$, by maximizing the joint distribution of the mono-static and bi-static observations. The direct approach is practically infeasible due to its high complexity. Instead, we propose a more efficient two-step method that first uses the delay and angle estimates from each individual system to determine initial target locations, which are subsequently refined via a data association and fusion step.

A. Mono-Static Location Estimation

For the mono-static system, the log likelihood is

$$g_{r,1}(\boldsymbol{\tau}_r, \boldsymbol{\theta}, \boldsymbol{\beta}) \propto -\|\boldsymbol{y}_r - \mathbf{H}_r \boldsymbol{\alpha}\|^2. \tag{15}$$

The MLE for $\boldsymbol{\alpha}$ is given by

$$\hat{\boldsymbol{\alpha}} = (\mathbf{H}_r^H \mathbf{H}_r)^{-1} \mathbf{H}_r^H \boldsymbol{y}_r. \tag{16}$$

Substituting $\hat{\boldsymbol{\alpha}}$ into the log likelihood, we have

$$g_{r,2}(\boldsymbol{\tau}_r, \boldsymbol{\theta}) \propto \boldsymbol{y}_r^H \mathbf{H}_r (\mathbf{H}_r^H \mathbf{H}_r)^{-1} \mathbf{H}_r^H \boldsymbol{y}_r \tag{17}$$

Thus, the MLE for target delays and DOAs can be obtained by a nonlinear least-squares fitting

$$\{\hat{\boldsymbol{\tau}}_r, \hat{\boldsymbol{\theta}}\} = \arg \max_{\boldsymbol{\tau}, \boldsymbol{\theta}} \boldsymbol{y}_r^H \tilde{\mathbf{H}}_r (\tilde{\mathbf{H}}_r^H \tilde{\mathbf{H}}_r)^{-1} \tilde{\mathbf{H}}_r^H \boldsymbol{y}_r. \tag{18}$$

Notice that the MLE for the delays and DOAs requires a $2K$-dimensional search, which is computationally intensive. For simplicity, instead of jointly estimating the delays and angles for K targets, we use a sequential method based on successive cancellation to estimate the delay and angle for one target at a time. That is, we start with estimating the strongest target, subtract it from the observation, and then use the residual to estimate the remaining targets by repeating the above process. Without loss of generality, we assume that the K targets are ordered such that $|\alpha_1| \geq \cdots \geq |\alpha_K|$. During the k-th step, we assume that residual $\boldsymbol{y}_r^{(k)}$ contains the k-th target and contributions from the remaining $K-k$ targets, which are treated as disturbance. The delay and angle for the k-th target can be obtained by

$$\{\hat{\tau}_{r,k}, \hat{\theta}_{r,k}\} = \arg \max_{\tau, \theta} |\boldsymbol{h}_r^H(\tau, \theta) \boldsymbol{y}_r^{(k)}|, \tag{19}$$

where $\boldsymbol{y}_r^{(k)} = \boldsymbol{y}_r^{(k-1)} - \hat{\alpha}_{k-1} \boldsymbol{h}_r(\hat{\tau}_{r,k-1}, \hat{\theta}_{r,k-1})$, and $\boldsymbol{y}_r^{(1)} = \boldsymbol{y}_r$. Once $\hat{\tau}_{r,k}$ and $\hat{\theta}_{r,k}$ are found, the amplitude can be computed by least squares

$$\hat{\alpha}_k = (\boldsymbol{h}_r^H(\hat{\tau}_{r,k}, \hat{\theta}_{r,k}) \boldsymbol{h}_r(\hat{\tau}_{r,k}, \hat{\theta}_{r,k}))^{-1} \boldsymbol{h}_r^H(\hat{\tau}_{r,k}, \hat{\theta}_{r,k}) \boldsymbol{y}_r^{(k)}.$$

Next, we discuss how to solve (19) efficiently by using 2-D FFT. The cost function in (19) can be written as

$$\sum_{q=1}^{N_R} \sum_{l=1}^{L_r} e^{j\pi(q-1)\sin\theta_k} e^{j2\pi(l-1)\tau_k^r \Delta f_r} \boldsymbol{s}_r^*(l) \boldsymbol{y}_{r,q,l}, \tag{20}$$

which can be viewed as a 2-D FFT of a matrix $\mathbf{Y}_r$ at frequencies $\frac{\sin\theta_k}{2} \in (-0.5, 0.5]$ and $-\tau_k^r \Delta f_r \in [-1, 0]$, where matrix $\mathbf{Y}_r \in \mathbb{C}^{L_r \times N_R}$ is given by

$$\mathbf{Y}_r[l, q] = \boldsymbol{s}_r^*(l) \boldsymbol{y}_{r,q,l},\ l = 1, \ldots, L_r,\ q = 1, \ldots, N_R.$$

Hence, τ_k^r and θ_k can be found by identifying the peak of the 2-D FFT magnitude. Assuming the peak location is $\{\hat{u}, \hat{v}\}$, we can calculate the delay and Doppler estimates by

$$\hat{\tau}_k^r = \frac{M_\tau - \hat{u} + 1}{M_\tau \Delta f}, \tag{21}$$

$$\hat{\theta}_{r,k} = \text{sign}(\kappa) \sin^{-1}\left(\frac{2(M_\theta/2 - |\kappa|)}{M_\theta}\right), \tag{22}$$

where "sign" denotes the sign function, $\kappa = (\hat{v} - 1) - M_\theta/2$, M_τ and M_θ the 2-D FFT grid numbers.

Once the target delays and angles estimates are obtained, the k-th target location can be calculated by

$$\begin{aligned} \hat{u}_{r,k}^x &= \tfrac{1}{2} c \hat{\tau}_k^r \cos(\hat{\theta}_{r,k}) + u_r^x, \\ \hat{u}_{r,k}^y &= \tfrac{1}{2} c \hat{\tau}_k^r \sin(\hat{\theta}_{r,k}) + u_r^y. \end{aligned} \tag{23}$$

B. Bi-Static Location Estimation

For the bi-static system, the delay and angle for each target can be estimated by using a similar sequential approach. We also assume that the targets are ordered, $|\beta_1| \geq \cdots \geq |\beta_K|$. Note that targets may have different orders in the two systems. During the k-th step, the delay and angle for the k-th target can be estimated from the residual $\boldsymbol{y}_c^{(k)}$:

$$\{\hat{\tau}_{c,k}, \hat{\theta}_{c,k}\} = \arg \max_{\tau, \theta} ||\boldsymbol{h}_c(\tau, \theta)^H \boldsymbol{y}_c^{(k)}||_2, \tag{24}$$

where $\boldsymbol{y}_c^{(k)} = \boldsymbol{y}_c^{(k-1)} - \hat{\beta}_{k-1} \boldsymbol{h}_c(\hat{\tau}_{c,k}, \hat{\theta}_{c,k})$, and $\boldsymbol{y}_c^{(1)} = \boldsymbol{y}_c$. The amplitude can be similarly obtained by least squares

$$\hat{\beta}_k = (\boldsymbol{h}_c(\hat{\tau}_{c,k}, \hat{\theta}_{c,k})^H \boldsymbol{h}_c(\hat{\tau}_{c,k}, \hat{\theta}_{c,k}))^{-1} \boldsymbol{h}_c(\hat{\tau}_{c,k}, \hat{\theta}_{c,k})^H \boldsymbol{y}_c^{(k)}.$$

Thus, the target delay and angle in (24) can also be estimated by computing the 2-D FFT of $\mathbf{Y_c}$ followed by the peak finding. The matrix $\mathbf{Y_c}$ can be obtained by $\mathbf{Y}_c[l, q] = \boldsymbol{s}_c^*(l) \boldsymbol{y}_{c,q,l},\ l = 1, \ldots, L_r,\ q = 1, \ldots, N_R$. Assuming the peak location on the 2-D FFT grid of the matrix $\mathbf{Y_c}$ is $\{\hat{u},' \hat{v}'\}$, we can calculate the delay and angle estimates by

$$\hat{\tau}_k^c = \frac{M_\tau - \hat{u}' + 1}{M_\tau \Delta f}, \tag{25}$$

$$\hat{\theta}_{c,k} = \text{sign}(\kappa') \sin^{-1}\left(\frac{2(M_\theta/2 - |\kappa'|)}{M_\theta}\right), \tag{26}$$

where $\kappa' = (\hat{v}' - 1) - M_\theta/2$.

After the delay and angle estimates are obtained, the k-th target locations estimation for bi-static system can be calculated by using the equation of ellipse whose focal points are at the receiver location $\boldsymbol{u}_r$ and the transmitter location $\boldsymbol{u}_c$ of the bi-static system:

$$\begin{aligned} \hat{u}_{c,k}^x &= \tfrac{\rho(1-\epsilon^2)}{1-\epsilon\cos\hat{\theta}_{c,k}} \cos\hat{\theta}_{c,k} + u_r^x, \\ \hat{u}_{c,k}^y &= \tfrac{\rho(1-\epsilon^2)}{1-\epsilon\cos\hat{\theta}_{c,k}} \sin\hat{\theta}_{c,k} + u_r^y, \end{aligned} \tag{27}$$

where $\rho = (c\hat{\tau}_k^c + ||\boldsymbol{u}_c||_2)/2$ and $\epsilon = \frac{||\boldsymbol{u}_c||_2}{c\hat{\tau}_k^c + ||\boldsymbol{u}_c||_2}$ denote the length of the semi-major axis and eccentricity for the ellipse, respectively.

C. Data Association and Fusion

Next, we discuss how to fuse the two sets of location estimates into the final one. Since the order may differ in the two initial location estimates, we propose a data association method based on minimizing the Euclidean distances between the initial location estimates. Denote the location vectors obtained by the mono-static and bi-static systems by $\boldsymbol{l}_r = [(\hat{u}^x_{r,1}, \hat{u}^y_{r,1}), \ldots, (\hat{u}^x_{r,K}, \hat{u}^y_{r,K})]$ and $\boldsymbol{l}_c = [(\hat{u}^x_{c,1}, \hat{u}^y_{c,1}), \ldots, (\hat{u}^x_{c,K}, \hat{u}^y_{c,K})]$, respectively. Then, a matrix $\mathbf{S_c} \in \mathbb{R}^{K \times M}$ is formed whose columns are obtained by permuting entries in $\boldsymbol{l}_c$ and $M = K!$ is the total number for permutations of $\boldsymbol{l}_c$. The association problem can be solved by finding the column of $\mathbf{S_c}$ which has the minimum Euclidean distance to $\boldsymbol{l}_r$

$$\min_{m=1,\ldots,M} \|\boldsymbol{l}_r - \mathbf{S_c}(:,m)\|_2, \tag{28}$$

where $\mathbf{S_c}(:,m)$ represents the m-th column of the matrix. The above exhaustive search based method has a complexity $\mathcal{O}(K!)$, which is feasible for small K. For larger K, we can use a simpler greedy association method. Specifically, the greedy method goes through the first set of target estimates (obtained by the mono-static system) one at a time, starting from the strongest target, then finds its best match from the second set of estimates (obtained by the bi-static system), and each time when a match is identified, it is removed for further comparison. The process is continued until all targets are matched up. It is clear the greedy has a complexity $\mathcal{O}(K^2)$.

Suppose after the association, the location estimates for the k-th target are denoted by $(\hat{u}^x_{r,k}, \hat{u}^y_{r,k})$ and $(\hat{u}^x_{c,\tilde{k}}, \hat{u}^y_{c,\tilde{k}})$ for the mono-static and bi-static system, respectively. Then the k-th target location can be obtained by a weighted combination of the two location estimates according to their relative strength/amplitude estimates:

$$(\hat{u}^x_k, \hat{u}^y_k) = \frac{|\hat{\alpha}_k|(\hat{u}^x_{r,k}, \hat{u}^y_{r,k}) + |\hat{\beta}_{\tilde{k}}|(\hat{u}^x_{c,\tilde{\boldsymbol{k}}}, \hat{u}^y_{c,\tilde{\boldsymbol{k}}})}{|\hat{\alpha}_k| + |\hat{\beta}_{\tilde{k}}|}. \tag{29}$$

IV. Simulation Results

In this section, we present numerical results to illustrate the performance of the cooperative mono-static and bi-static sensing system. Consider a case where the Vehicle 1 is located at $(0\,m, 0m)$ and Vehicle 2 is located at $(30\,m, 0m)$. The bandwidth for both systems system is 150 MHz and the maximum range is 50 m [8], [9], [22]. Pseudo random spreading codes with length $L_r = L_c = L = 50$ are employed for both systems. The number of antennas for both systems are $N = 10$. The signal-to-noise ratio (SNR) for the mono-static and bi-static systems are defined as

$$\text{SNRr} = |\alpha_1|^2/\sigma^2, \quad \text{SNRc} = |\beta_1|^2/\sigma^2. \tag{30}$$

Suppose there are 4 targets with locations $(15.81\,m, 11.87\,m)$, $(35.92\,m, 5.86\,m)$, $(21.7\,m, -18.48\,m)$, and $(33.8\,m, -25.3\,m)$ in the considered area with the amplitudes ratio $|\alpha_1| : |\alpha_2| : |\alpha_3| : |\alpha_4| = |\beta_1| : |\beta_2| : |\beta_3| : |\beta_4| = 1 : 0.8 : 0.6 : 0.4$.

Fig. 2(a) to 2(c) show results for one simulation trial of the target location estimates obtained by using only the mono-static

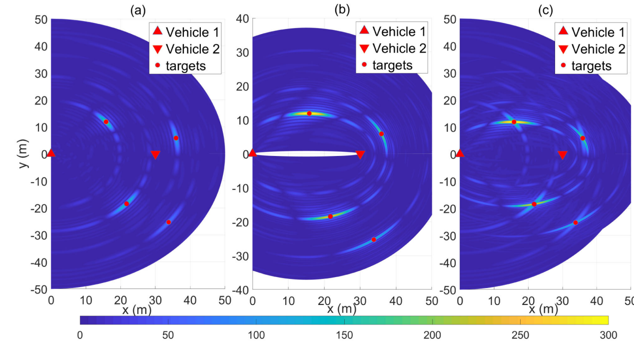

Fig. 2. Target location images obtained by (a) mono-static, (b) bi-static, and (c) cooperative sensing system when SNRr = 25 dB and SNRc = 30 dB.

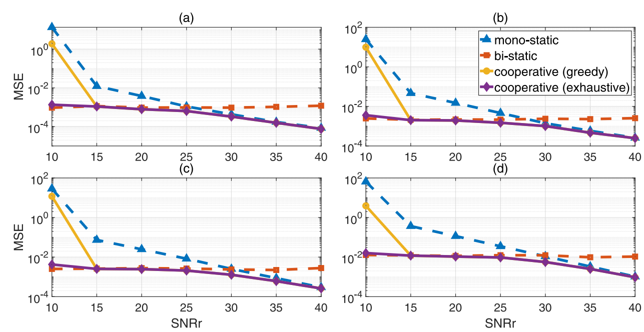

Fig. 3. MSE versus SNRr with SNRc = 30 dB: (a) target 1; (b) target 2; (c) target 3; (d) target 4.

system, only the bi-static system, and the cooperative mono-static and bi-static systems, respectively, when SNRr = 25 dB and SNRc = 30 dB. The results shows that the target locations can be determined by using only the mono-static or bi-static sensing system with the proposed sequential approach discussed in Sections III-A and III-B. Fig. 2(c) shows that with the help of the cooperation, the target location estimates are refined with a higher resolution by finding the intersection of the initial target location estimates in two systems.

Next, Fig. 3 shows the mean squared error (MSE) of the target location estimates which are obtained via 200 independent trials. It is seen that the MSE of the cooperative mono-static and bi-static system is smaller than the MSE of mono-static sensing system and the difference between them decrease as SNRr increase. It is also seen that, compared with the exhaustive search, the greedy based association results in some degradation at low SNR.

V. Conclusion

We proposed an efficient method to localize multiple targets by using a cooperative mono-static and bi-static system for the automotive sensing. The initial target locations are calculated by using the delay and DOA estimates which are obtained in each system via peak finding on the 2-D FFT grid of the observations. Then, a data association and fusion method is used to refine the target estimates. Simulation results show that the bi-static system can help the mono-static system to find better target location estimates in terms of the MSE especially when the bi-static system has a sufficiently high SNR.

REFERENCES

[1] H. H. Meinel, "Evolving automotive radar - From the very beginnings into the future," in *Proc. 8th Eur. Conf. Antennas Propag.*, 2014, pp. 3107–3114.

[2] S. Sun, A. P. Petropulu, and H. V. Poor, "MIMO radar for advanced driver-assistance systems and autonomous driving: Advantages and challenges," *IEEE Signal Process. Mag.*, vol. 37, no. 4, pp. 98–117, Jul. 2020.

[3] J.-J. Lin, Y.-P. Li, W.-C. Hsu, and T.-S. Lee, "Design of an FMCW radar baseband signal processing system for automotive application," *SpringerPlus*, vol. 5, no. 1, pp. 1–16, 2016.

[4] J. Hasch, E. Topak, R. Schnabel, T. Zwick, R. Weigel, and C. Waldschmidt, "Millimeter-wave technology for automotive radar sensors in the 77 GHz frequency band," *IEEE Trans. Microw. Theory Techn.*, vol. 60, no. 3, pp. 845–860, Mar. 2012.

[5] J. Choi, V. Va, N. Gonzalez-Prelcic, R. Daniels, C. R. Bhat, and R. W. Heath, "Millimeter-wave vehicular communication to support massive automotive sensing," *IEEE Commun. Mag.*, vol. 54, no. 12, pp. 160–167, Dec. 2016.

[6] I. Bilik, O. Longman, S. Villeval, and J. Tabrikian, "The rise of radar for autonomous vehicles: Signal processing solutions and future research directions," *IEEE Signal Process. Mag.*, vol. 36, no. 5, pp. 20–31, Sep. 2019.

[7] K. V. Mishra, M. Bhavani Shankar, V. Koivunen, B. Ottersten, and S. A. Vorobyov, "Toward millimeter-wave joint radar communications: A signal processing perspective," *IEEE Signal Process. Mag.*, vol. 36, no. 5, pp. 100–114, Sep. 2019.

[8] S. M. Patole, M. Torlak, D. Wang, and M. Ali, "Automotive radars: A review of signal processing techniques," *IEEE Signal Process. Mag.*, vol. 34, no. 2, pp. 22–35, Mar. 2017.

[9] S. Alland, W. Stark, M. Ali, and M. Hegde, "Interference in automotive radar systems: Characteristics, mitigation techniques, and current and future research," *IEEE Signal Process. Mag.*, vol. 36, no. 5, pp. 45–59, Sep. 2019.

[10] Z. Xu and Q. Shi, "Interference mitigation for automotive radar using orthogonal noise waveforms," *IEEE Geosci. Remote Sens. Lett.*, vol. 15, no. 1, pp. 137–141, Jan. 2018.

[11] A. J. Weiss, "Direct geolocation of wideband emitters based on delay and doppler," *IEEE Trans. Signal Process.*, vol. 59, no. 6, pp. 2513–2521, Jun. 2011.

[12] C.-H. Park and J.-H. Chang, "Closed-form localization for distributed MIMO radar systems using time delay measurements," *IEEE Trans. Wireless Commun.*, vol. 15, no. 2, pp. 1480–1490, Feb. 2016.

[13] X. Zhang, F. Wang, H. Li, and B. Himed, "Maximum likelihood and IRLS based moving source localization with distributed sensors," *IEEE Trans. Aerosp. Electron. Syst.*, vol. 57, no. 1, pp. 448–461, Feb. 2021.

[14] Y. Sun, K. C. Ho, and Q. Wan, "Eigenspace solution for AOA localization in modified polar representation," *IEEE Trans. Signal Process.*, vol. 68, pp. 2256–2271, 2020.

[15] T. Jia, H. Wang, X. Shen, Z. Jiang, and K. He, "Target localization based on structured total least squares with hybrid TDOA-AOA measurements," *Signal Process.*, vol. 143, pp. 211–221, 2018.

[16] Y.-Y. Li, G.-Q. Qi, and A.-D. Sheng, "Performance metric on the best achievable accuracy for hybrid TOA/AOA target localization," *IEEE Commun. Lett.*, vol. 22, no. 7, pp. 1474–1477, Jul. 2018.

[17] S. H. Dokhanchi, B. S. Mysore, K. V. Mishra, and B. Ottersten, "A mmWave automotive joint radar-communications system," *IEEE Trans. Aerosp. Electron. Syst.*, vol. 55, no. 3, pp. 1241–1260, Jun. 2019.

[18] S. H. Dokhanchi, M. R. Bhavani Shankar, K. V. Mishra, T. Stifter, and B. Ottersten, "Performance analysis of mmWave bi-static PMCW-based automotive joint radar-communications system," in *Proc. IEEE Radar Conf.*, 2019, pp. 1–6.

[19] X. Zhang, H. Li, and B. Himed, "Maximum likelihood delay and doppler estimation for passive sensing," *IEEE Sensors J.*, vol. 19, no. 1, pp. 180–188, Jan. 2019.

[20] M. S. Greco and A. De Maio, *Modern Radar Detection Theory*. London, U.K.: Inst. Eng. Technol., 2015.

[21] T. Tian, T. Zhang, L. Kong, G. Cui, Q. Shi, and Y. Deng, "Performance of localization estimation rate for radar-communication system," in *Proc. IEEE Radar Conf.*, 2019, pp. 1–6.

[22] F. Liu, C. Masouros, A. P. Petropulu, H. Griffiths, and L. Hanzo, "Joint radar and communication design: Applications, state-of-the-art, and the road ahead," *IEEE Trans. Commun.*, vol. 68, no. 6, pp. 3834–3862, Jun. 2020.